JOURNAL OF SPACECRAFT AND ROCKETS
Vol. 29, No. 1, January-February 1992

Defining Orbital Debris Environmental Conditions for Spacecraft Vulnerability Assessment

Robert C. Reynolds*
System Planning Corporation, Houston, Texas 77058
and
Gregory W. Ojakangas† and Phillip D. Anz-Meador‡
Lockheed Engineering & Sciences Company, Houston, Texas 77058

The major problem that orbital debris presents to a particular space structure is not that of catastrophic collision, which fragments the structure, but rather the threat of collisions with small debris that will damage it. In this paper, a method is developed for defining the debris environment to support the analysis of vulnerability of space structures. Flux directionality functions related to spacecraft surface degradation, which are seen to be various velocity moments of the phase space debris density distribution, are derived for both the man-made debris environment and for a simple model of the meteoroid environment. A method for accounting for the shielding of spacecraft surfaces by other spacecraft components is also presented within the flux directionality context.

Nomenclature

C_ξ = cos ξ
D_k = kth cumulative mass moment of $\mathfrak{D}$
$\mathfrak{D}$ = differential size distribution
$d\Omega$ = differential element of solid angle
$\mathfrak{F}$ = number flux density, impacts/km^2/s/sr
$\mathfrak{F}_a$ = crater area flux density, cm^2/km^2/s/sr
$\mathfrak{F}_e$ = kinetic energy flux density, erg/km^2/s/sr
$\mathfrak{F}_m$ = cumulative mass flux density, g/km^2/s/sr
$\mathfrak{F}_{vol}$ = crater volume flux density, cm^3/km^2/s/sr
h_o = spacecraft altitude
i = debris incidence angle (i.e., angle of debris impact relative to a spacecraft surface element)
n = number density, /km^3
q = phase space mass density distribution
R_E = radius of Earth
r = position
S_ξ = sin ξ
v = velocity, km/s
v_{sc} = spacecraft velocity in an Earth-centered inertial reference frame
γ = angle between spacecraft velocity vector and debris velocity vector in an Earth-centered inertial reference frame
η = phase space number density, /km^6/s^3
θ = yaw angle (angle in local horizontal plane)
ρ = mass density, g/cm^3
φ = pitch angle (angle out of local horizontal plane)
φ_E = pitch angle of Earth's limb in local vertical local horizontal reference frame
φ_{sc} = pitch angle of spacecraft velocity vector
ν = ratio of spacecraft velocity to particle velocity in an Earth-centered inertial reference frame

Subscripts
c = reference frame co-moving with spacecraft
m = meteoroid
o = Earth-centered inertial reference frame
s = spacecraft surface

Introduction

ALTHOUGH orbital debris environment investigations have tended to focus on the catastrophic breakups that control the growth of the debris environment, the issue for particular space programs or designers/operators of individual spacecraft is collisions with smaller objects that will damage a space structure. In some cases this threat is already of concern, and is growing as activity in space increases. To understand the debris threat arising from these damaging collisions it is necessary to define the direction, size, and velocity distributions of the debris relative to the spacecraft surfaces. It is also essential to understand the consequences of an impact on the space structure; the emphasis in this paper, however, is to develop a very useful method for defining the environment.

In this paper distributions of particles over the velocity coordinates of the six-dimensional phase space defined by position and velocity are used to provide a generalized context for discussing the environmental characteristics for both the man-made and meteoroid environments. In this formulation, the flux density is the velocity moment of the phase space number density distribution integrated over velocity magnitude[1] and is more properly referred to as the number flux density function. Other velocity moments of the phase space number density can be defined for surface damage, impact hole formation, and the like. These functions are defined for both meteoroids and man-made debris to provide a demonstration of the methodology and to indicate a means of interpreting the relative contribution of man-made debris and meteoroids on returned spacecraft surfaces such as the long duration exposure facility (LDEF). The combined environments are interpreted for oriented surfaces.

A second major issue to be addressed for spacecraft vulnerability is the shielding of spacecraft surfaces by other spacecraft components and the complementary formation of a secondary fragment flux. At a given point on the spacecraft structure, other elements of that structure will occupy a portion of the 4π sr as seen by that point. For a simple convex

Presented as Paper 90-3862 at the AIAA Space Programs and Technologies Conference, Huntsville, AL, Sept. 25-28, 1990; received Nov. 19, 1990; revision received May 18, 1991; accepted for publication May 24, 1991.

*Director, Orbital Debris Studies.
†Scientist.
‡Principal Scientist.

structure, as discussed in Ref. 1, this will be 2π sr. However, for complex structures there will be additional elements in the field of view. These elements will shield the surface from the primary flux, but may, in the process, act as a source of secondaries. A simple model portraying this effect is introduced in this paper.

In summary, this paper will present two significant developments for orbital debris modeling: 1) a technique using various flux densities of the debris environment to account for spacecraft surface degradation and surface penetrability effects that is applied to oriented spacecraft surfaces for both the man-made and meteoroid environments, and 2) a method within the flux density formalism to account for shielding of spacecraft surfaces by other spacecraft structures for geometrically complex spacecraft.

Discussion

Phase Space Distribution Functions

The phase space, as defined in this paper, is the six-dimensional space that has position and velocity as coordinates. In this space, let $\eta(r,v)$ denote the phase space number density function. That is, the number of objects in a phase space volume element centered on (r_o,v_o), $dN(r_o,v_o)$, will be

$$dN(r_o,v_o) = \eta(r_o,v_o)\, d^3r d^3v \tag{1}$$

The number density in physical space, $n(r_o)$, will be

$$n(r_o) = \int_v \eta(r_o,v)\, d^3v = \int_{4\pi} d\Omega \int_0^\infty \eta(r_o,v) v^2\, dv \tag{2}$$

In all further discussions, only the velocity characteristics will play a prominent role; it should be understood that all expressions are defined at some point r_o. Therefore, to simplify the mathematical expressions, the position argument will be suppressed in the following discussion.

Various interesting properties of an ensemble of particles can be defined from moments and integrals of this basic function η. The flux density function is the velocity weighted mean integrated over velocity magnitude.[1]

A local vertical local horizontal (LVLH) reference frame co-moving with the spacecraft will be used to define directions, yaw, and pitch relative to the spacecraft surfaces. The $+Z$ axis points to the zenith, the $+X$ axis in the orbital plane points in the direction of motion, and the $+Y$ axis points in the direction of the orbit angular momentum vector. In this coordinate system, yaw is measured clockwise in the local horizontal plane; 0-deg yaw is in the orbital plane in the direction of motion, and pitch is the angle out of the horizontal plane, where positive pitch denotes directions above the horizontal plane. In circular orbit, the velocity vector points to 0 deg in both yaw and pitch. Most spacecraft in low Earth orbit are in a fixed LVLH attitude. Therefore, the flux map in this coordinate system will reflect the exposure of the surface.

Expanding the notation for η,

$$\eta(v_o) = \eta(v_o,\theta_o,\varphi_o) \tag{3}$$

and letting the velocity volume element become

$$d^3v = v_o^2 C\varphi_o\, dv\, d\theta_o\, d\varphi_o \tag{4}$$

Further, letting $\hat{e}_{\Omega_o}$ be the unit vector pointing in the direction specified by (θ_o,φ_o), the flux density distribution, more properly called the number flux density $\mathfrak{F}$, is

$$\mathfrak{F}(\theta_o,\varphi_o) = \mathfrak{F}(\theta_o,\varphi_o)\hat{e}_{\Omega_o} = \hat{e}_{\Omega_o}\int_0^\infty \eta(v,\theta_o,\varphi_o) v^3\, dv \tag{5}$$

or

$$\mathfrak{F}(\theta_o,\varphi_o) = \int_0^\infty \eta(v,\theta_o,\varphi_o) v^3\, dv \tag{6}$$

Consider what happens in a frame moving at velocity v_{sc} relative to the frame used to define v_o. In this reference frame the phase space distribution function will be given by

$$\eta_c(v_c) = \eta_c(v_o - v_{sc}) = \eta(v_o) \tag{7}$$

For the most general case, v_c, θ_c, and φ_c are related to v_o, θ_o, and φ_o by

$$v_c = v_c \begin{pmatrix} C_{\theta_c} C_{\varphi_c} \\ S_{\theta_c} C_{\varphi_c} \\ S_{\varphi_c} \end{pmatrix} = v_o - v_{sc} \tag{8}$$

or

$$v_c \begin{pmatrix} C_{\theta_c} C_{\varphi_c} \\ S_{\theta_c} C_{\varphi_c} \\ S_{\varphi_c} \end{pmatrix} = \begin{pmatrix} v_o C_{\theta_o} C_{\varphi_o} - v_{sc} C_{\varphi_{sc}} \\ v_o S_{\theta_o} C_{\varphi_o} \\ v_o S_{\varphi_o} - v_{sc} S_{\varphi_{sc}} \end{pmatrix} \tag{9}$$

where $\varphi_{sc} = 0$ deg for circular orbits and where the fact that the yaw angle of the spacecraft velocity vector is by definition 0 deg has been used.

In this paper, the assumption will be made that the spacecraft will be moving in a circular orbit. Under this condition the velocity in the co-moving frame is related to the velocity in the inertial frame by

$$v_c^2 = v_o^2(1 + v^2 - 2vC_{\gamma_o}) \tag{10}$$

where $C_{\gamma_o} = C_{\theta_o} C_{\varphi_o}$ and γ_o is the cone angle in inertial space centered on the direction of spacecraft motion. At a given relative velocity, this conical surface is also a surface of constant central angle γ_c in the co-moving frame. The relation between γ_c and γ_o is given by

$$\frac{S_{\gamma_c}}{v_o} = \frac{S_{\gamma_o}}{v_c} \tag{11}$$

This means that the conditions found on a circle of angular radius γ_o that is centered on the direction of spacecraft motion in inertial space will map into a circle of angular radius γ_c that is also centered on this same direction. The circles in inertial space will always be translated forward in the co-moving frame so that there will be a concentration of objects coming from the direction of motion and a rarefaction in the direction away from that motion. However, as v_o increases, this effect decreases.

Flux Characteristics for a Simple Meteoroid Model

For the purposes of this paper, a rather simple meteoroid model will be used. The velocity distribution will be taken from the work of Southworth and Sekanina[2] and will be taken to be spherically symmetric, except for Earth shielding, in an inertial frame fixed on the Earth.

The volume covered by the velocity component of the phase space density function will be a sphere extending from a minimum velocity, assumed to be 11 km/s, to a maximum velocity, assumed to be 72 km/s. The Earth shielding will remove a conical section, centered on the nadir and extending out to a pitch angle given by

$$\varphi_E = -\cos^{-1}\left[R_E/(R_E + h_o)\right] \tag{12}$$

An orbit altitude of 800 km will be assumed, yielding φ_E of -27.31 deg.

The cutout for Earth shielding makes the integrals over the volume complex, and so all integrations have been performed numerically. This has the advantage that any distribution function, and any moment of that distribution function, can be handled with equal ease.

Hypervelocity impact effects on a spacecraft surface will depend on both the mass and relative velocity characteristics of the incident meteoroids, which may be related in a seven-dimensional phase plus mass space, as well as intrinsic characteristics of the two materials. It is the purpose of this paper to illustrate the characteristics of this phase plus mass space part of the penetration equations.

The phase space mass density distribution q, where $q(d_o,v_o)$ is defined to be the mass of objects per unit diameter interval centered on d_o per unit volume element of phase space, is related to the phase space number density distribution function η by the expression

$$q(d_o,v_o) = m(d_o)\mathfrak{D}(d_o)\eta(v_o) \tag{13}$$

where $m(d_o)$ is the mass of a meteoroid of diameter d_o. Both mass and velocity will enter the debris exposure expressions with various powers, depending on the penetration characteristic of interest. Defining a general functional form

$$D_k(d_o) = \int_{d_o}^{\infty} m^k(x)\mathfrak{D}(x)\,dx \tag{14}$$

with the normalization condition that $D_0(d_{\min}) = 1.0$, where $d_{\min}$ is the minimum size meteoroid of interest, provides a general form needed in the following discussion.

Work by many authors using various materials and various impact characteristics have shown that the impactor kinetic energy is a fundamental quantity. For example, the kinetic energy exponent for penetration depth is 0.357[3] or 0.333,[4-10] the exponent for crater diameter is 0.370[3] or 0.333,[5,7,9,10] and for crater volume it is 1.133.[3] Gault's work in Ref. 3 is for impact into dense crystalline rock, whereas the other references discuss impact into typical spacecraft materials. The results for spacecraft materials have been discussed and summarized by Schonberg and Taylor.[11] As can be seen, even from these diverse materials there is great similarity in the sensitivity to impactor kinetic energy.

In his work on impact into rock, Gault[3] also derived a functional dependence on the sine of the incidence angle.[3] This relationship will be needed when the exposure is calculated onto oriented spacecraft surfaces. In consequence, the exponents in the work of Gault will be used in this paper. Other, more general, relationships between mass and impact velocity have been found by other authors and could be used with ease in this approach, where the k value for D would change, as would the weighting of v in the velocity expressions.

In debris analysis fluxes are generally expressed in units of km^{-2}-s^{-1} or in m^{-2}-yr^{-1}. In keeping with this convention, the flux densities will be expressed in cgs units for the quantity transported and in units of km^{-2}-s^{-1}-(solid angle)$^{-1}$ for the flux density. This amounts to working in units of km/s for the velocities.

Four moment equations will be used to describe the exposure of the spacecraft surface to the meteoroid environment. These are the mass and kinetic energy flux density, and crater area and crater volume flux densities, quantities that characterize the degradation of a spacecraft surface and the amount of secondary debris created by impacts with meteoroids. The last two quantities assume that the crater depth is small relative to the thickness of the spacecraft surface material over those meteoroid sizes where there is significant contribution to the crater area or crater volume.

The choice of the crater area and crater volume functions implies that the resulting flux density functions are appropriate for the assessment of surface degradation of the outer spacecraft surface and are not the functions appropriate for assessment of penetration of this surface. For penetration assessment weighting functions would need to be defined for crater depth, but this problem is also more complicated since shielded and unshielded surfaces exhibit significantly different penetration behavior.

The mass flux density of meteoroids of diameter d_o or larger is

$$\mathfrak{F}_m = D_1(d_o)\int_0^{\infty} \eta v^3\,dv \tag{15}$$

When integrated over solid angle, it is the flux onto a sphere per unit cross-sectional area per unit time.

The energy flux density for meteoroids of diameter d_o or larger is,

$$\mathfrak{F}_e = D_1(d_o)\times 10^{10}\int_0^{\infty} \eta(0.5v^2)v^3\,dv$$

$$= 5.0\times 10^9 D_1(d_o)\int_0^{\infty} \eta v^5\,dv \tag{16}$$

When integrated over solid angle, $\mathfrak{F}_e$ gives the energy flux onto a sphere per unit cross-sectional area per unit time, again for meteoroids to a limiting size of d_o.

Gault[3] presents an expression for the average diameter of an impact feature d_a, which will be simply related to the impact crater area by assuming the crater is circular. Under these conditions, using the terminology of this paper, the crater area flux density $\mathfrak{F}_a$ will be

$$\mathfrak{F}_a = 26.69(\rho_m\rho_s^{-3})^{1/3}D_{0.740}(d_o)S_i^{1.720}\int_0^{\infty} \eta v^{4.480}\,dv \tag{17}$$

where $\mathfrak{F}_a$ is the spacecraft surface area cratered by objects larger than d_o in diameter per unit time when integrated over solid angle. If the spacecraft surface was a brittle material, this function should be scaled up by at least an order of magnitude.

Similarly, the volume of spacecraft surface material ejected can be derived from Gault's expression for displaced mass. The form for this ejecta volume flux density, $\mathfrak{F}_{\text{vol}}$, is

$$\mathfrak{F}_{\text{vol}} = 8.471(\rho_m\rho_s^{-3})^{0.5}D_{1.133}(d_o)S_i^2\int_0^{\infty} \eta v^{5.266}\,dv \tag{18}$$

where $\mathfrak{F}_{\text{vol}}$ is the volume of spacecraft surface cratered out per unit area per unit time when integrated over solid angle.

In performing the integrals over solid angle for $\mathfrak{F}_a$ and $\mathfrak{F}_{\text{vol}}$, i will be related to both the integration variables and the surface normal vector. If θ_s refers to yaw and φ_s the pitch for the surface normal vector, the angle between this vector and one directed to (θ_c,φ_c) will be given by

$$\alpha = \cos^{-1}\left[C(\theta_c-\theta_s)C_{\varphi_c}C_{\varphi_s} + S_{\varphi_c}S_{\varphi_s}\right] \tag{19}$$

and $i = 90\text{ deg} - \alpha$. In performing the integration, only positive angles for i are used. It should be noted that Gault states that his relationships may break down for $i < 15$ deg, but this effect is not considered in this paper.

The probability distribution for meteoroids being in velocity interval v to $v + dv$ was taken from Zook[12] and has functional form

$$P(v) \propto 10^{-0.1072v} \tag{20}$$

in all directions except where the Earth shields the environment. This probability distribution yields a phase space number density distribution function of form

$$\eta(v_c) = K_0\times 10^{-0.1072v_o(v_c)}v_o^{-3}(v_c) \tag{21}$$

where K_0 is a constant determined from observational data. The observed cumulative surface area flux for the meteoroid population as a function of meteoroid size at altitude 500 km[13] is approximated by

$$F_s^{500}(d) = 1.6795\times 10^{-8}d^{-3.66}(\text{km}^{-2}\text{-s}^{-1}) \quad d > 0.01\text{ cm} \tag{22}$$

where d is expressed in centimeters. The standard relation of surface area flux being one-fourth the cross-sectional area flux F_x leads to

$$F_x^{500}(d) = 6.718 \times 10^{-8} d^{-3.66} (\text{km}^{-2}\text{-s}^{-1}) \tag{23}$$

The cross-sectional area flux may be defined in terms of the distribution functions by

$$F_x(d) = D_0(d) \int \eta v^3 \, dv \, d\Omega \tag{24}$$

For the size distribution implied by Eq. (22),

$$\mathfrak{D}(d) = K_1 d^{-4.66} \qquad d > 0.01 \text{ cm} \tag{25}$$

so that $K_1 = 1.75 \times 10^{-7}$ to satisfy the normalization condition that $D_0(0.01) = 1.0$, and

$$D_0(d) = 4.786 \times 10^{-8} d^{-3.66} \tag{26}$$

Performing the integration of Eq. (24) numerically for an orbit altitude of 500 km leads to

$$K_0 = 1.69 \times 10^{-4} \tag{27}$$

and η becomes

$$\eta(v_c) = 1.69 \times 10^{-4} 10^{-0.1072 v_o(v_c)} v_o^{-3}(v_c) \tag{28}$$

where the altitude dependence enters through the angular size of the Earth, as expressed indirectly in Eq. (12).

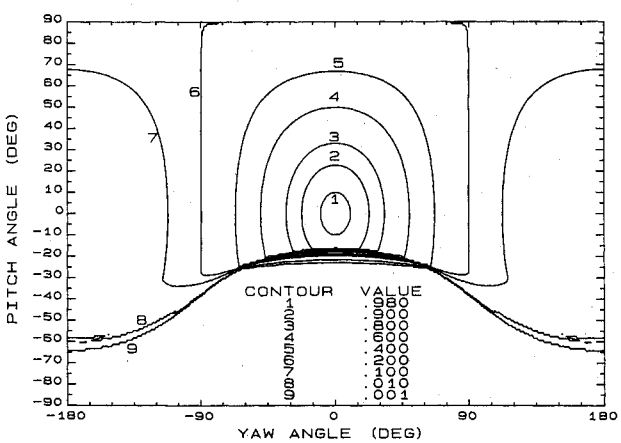

Fig. 1 Relative number or mass flux density for meteoroid environment.

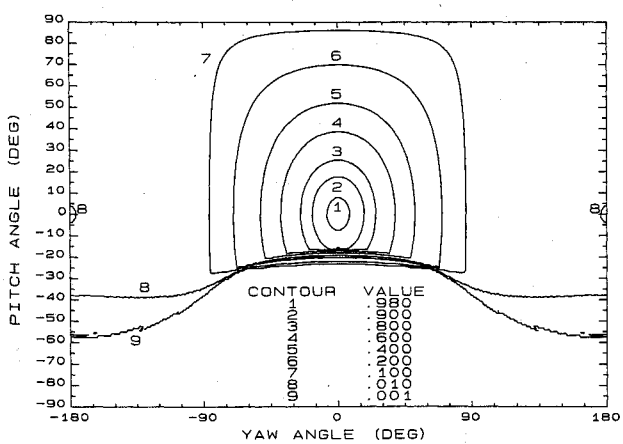

Fig. 2 Relative energy flux density for meteoroid environment.

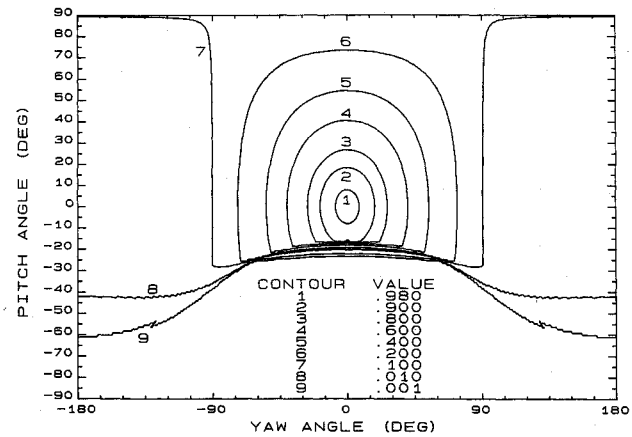

Fig. 3 Relative crater area flux density for meteoroid environment.

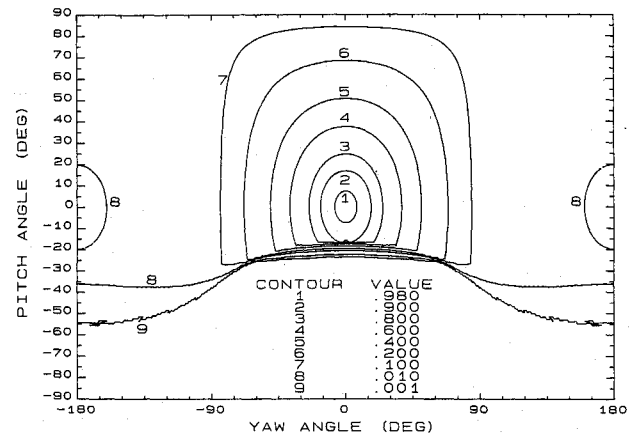

Fig. 4 Relative ejecta volume flux density for meteoroid environment.

Using this distribution function, and a spacecraft orbit altitude of 800 km, the four velocity integrals, as defined in Eqs. (13–16), are plotted as a function of direction in Figs. 1–4.

The moment equations needed to evaluate the complete expressions for these equations are expressible for a general k value as

$$D_k(d_o) = \frac{1.75 \times 10^{-7}}{(3.66 - 3k)} \left(\frac{\pi \rho_m}{6} \right)^k d_o^{3k-3.66} \tag{29}$$

where the meteoroids have been assumed to be spherical, and it has been assumed that $k < 3.66/3$, which is the case for all of the functions used.

Flux Characteristics for the Man-Made Debris Environment

In contrast to the phase space distribution of the meteoroids, that for the man-made debris environment will form a thin shell in the velocity and pitch directions, driven by the eccentricity distribution, and a broad but irregular distribution in the yaw direction, driven by the inclination distribution. It is a function derivable from the inclination and eccentricity distribution, given the assumption of a random distribution in right ascension of ascending node and argument of perigee for the debris, but in fact this derivation has not been performed. Rather, the distribution has been derived numerically for the set of observed objects and extrapolated to smaller objects based on the expected relative spatial densities based on modeling. The size distribution is taken from the standard orbital debris design environment.[14]

The result of this modeling is shown in the mass flux density plot of Fig. 5 for an 800-km orbit of 98.0-deg inclination.

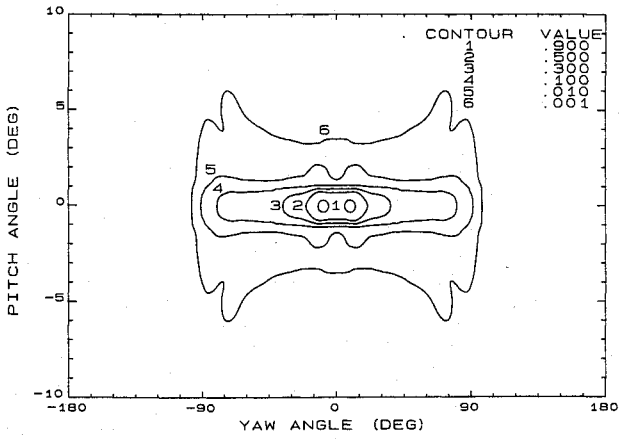

Fig. 5 Relative number or mass flux density for man-made debris.

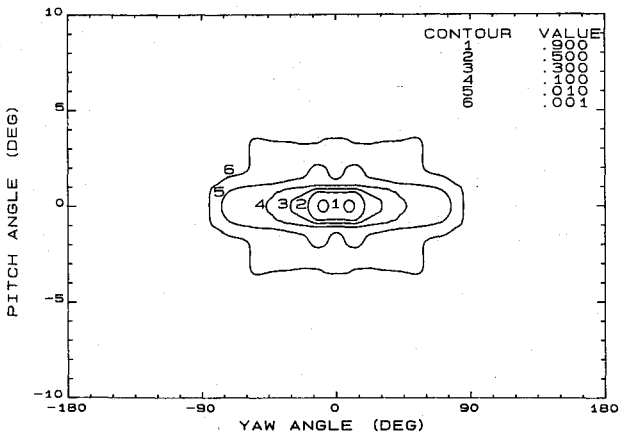

Fig. 6 Relative energy flux density for man-made debris.

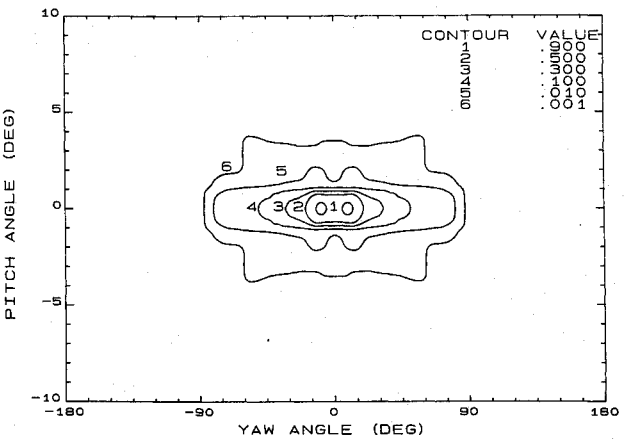

Fig. 7 Relative crater area flux density for man-made debris.

Using the same moments to generate flux density as was used for the meteoroid population, the corresponding energy flux density, crater area flux density, and ejecta mass flux density velocity integrals are shown in Figs. 6-8. The pitch scale has been expanded for these figures since impacts with man-made debris occur very nearly in the local horizontal plane for a spacecraft in circular orbit.

Comparison of the Meteoroid and Man-Made Debris Environments

The differences in the distribution functions for the two environments are obviously significant, as can be seen in Figs. 1-8. Table 1 presents the cumulative flux levels for the two populations as a function of size, where a projected man-made population for 1995 has been used, and Fig. 9 shows the details in the contrasting distributions along the 0-deg pitch line as a function of yaw for the two populations for sizes 100 μ and larger. This path in LVLH space contains the maximum contribution from both populations. Since all of the functions are symmetric in yaw, only yaw values from 0 to 180 deg are shown. As indicated in Table 1, the meteoroid population is increasing with decreasing size more rapidly than the man-made environment, and so, at larger sizes, the meteoroid curve will drop relative to the man-made debris curve.

A complete description of the combined environments is shown in Fig. 10 for the number flux for the 100-μ and larger environment. As was indicated in Fig. 9, this environment is dominated by the man-made environment near the horizontal plane, but away from this plane only the meteoroids contribute.

The differences in distribution functions becomes even more apparent when the effects on oriented surfaces is considered. Six surface orientations were considered, as defined by the location of the surface normal vector in Table 2, and the relative effects on these surfaces were considered for the four functions defined in Eqs. (15-18). It was assumed that the

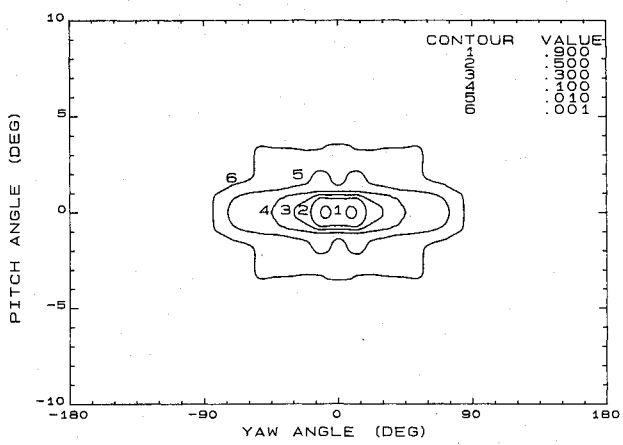

Fig. 8 Relative ejecta volume flux density for man-made debris.

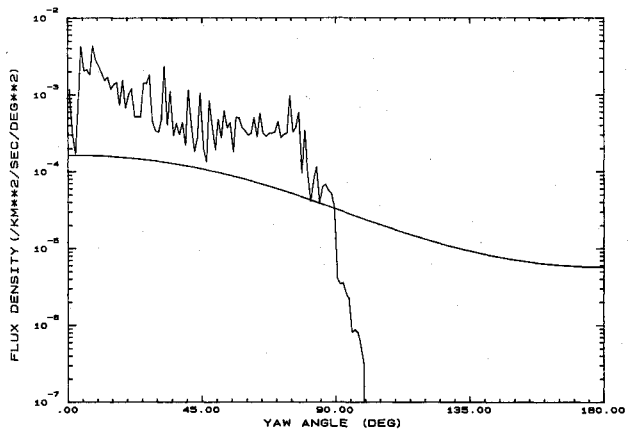

Fig. 9 Number flux density distribution for 0-deg pitch angle for both the man-made and meteoroid 100-μ environments.

Table 1 Cross-sectional flux levels as a function of debris size (impacts/km^2/s)

Debris size, cm	Man made	Meteoroid
10.0	1.06×10^{-7}	1.55×10^{-11}
1.0	3.36×10^{-6}	7.11×10^{-8}
0.1	8.90×10^{-4}	3.26×10^{-4}
0.01	0.283	1.499

Table 2 Six surface orientations

Name	Pitch, deg	Yaw, deg
Front	0	0
Top	90	0
Bottom	−90	0
Left side	0	90
Right side	0	−90
Back	0	−180

Table 3 Relative effect of flux functions on oriented surfaces for the meteoroid environment

Surface	Mass	Energy	Crater area	Ejecta volume
Front	1.000	1.000	1.000	1.000
Top	0.577	0.433	0.459	0.422
Bottom	0.122	0.091	0.095	0.090
Side	0.451	0.339	0.358	0.330
Back	0.119	0.045	0.055	0.042

Table 4 Relative effect of flux functions on oriented surface for the man-made environment

Surface	Mass	Energy	Crater area	Ejecta volume
Front	1.000	1.000	1.000	1.000
Top	0.007	0.005	10^{-5}	$<10^{-5}$
Bottom	0.007	0.005	10^{-5}	$<10^{-5}$
Side	0.259	0.163	0.068	0.045
Back	$<10^{-3}$	$<10^{-5}$	$<10^{-5}$	$<10^{-5}$

Table 5 Relative mass flux for the combined meteoroid and debris environments at three limiting sizes

Surface	0.1 mm	1 mm	1 cm
Front	1.000	1.000	1.000
Top	0.451	0.119	0.015
Bottom	0.096	0.029	0.008
Side	0.410	0.296	0.261
Back	0.093	0.023	0.002

surface was shielded only from below by the surrounding surface; that is, each surface was exposed to 2π sr of deep space. The relative contributions are shown relative to the front surface exposure in all cases.

With the simple shielding assumed for these calculations, there is yaw symmetry about 0 deg, so that the left and right side exposures are the same, and only one number is provided for the side face.

The meteoroid environment is presented in Table 3. The mass flux is found to be greatest on the top surface, which might not be expected since the front surface is partially shielded by the Earth. This specific result is a function of the velocity distribution for the meteoroids, but will be true in general since the meteoroids are moving much faster than the spacecraft. For this same reason, there is a significant flux onto the Earth-facing (bottom) and back-facing surfaces.

Table 4 synopsizes the flux seen by these same surfaces for the man-made environment. The much more confined distributions characterizing this environment are seen in the dramatic reduction in exposure of the top, bottom, and back surfaces, although the causes of this are different. The reduction in flux on the top and bottom surfaces is a reflection of the concentration of debris flux near 0-deg pitch angle; a significant component of this flux will be high-velocity particle moving at very low impact angles to the surface. The reduction in flux on the back face is a reflection of the fact that man-made debris is at almost the same speeds, so that there is very little debris that can catch up with the spacecraft; all of the flux on this surface will be low speed, i.e., <2 km/s.

Three cases for the combined environment are shown in Table 5. The mass flux is used, and the exposures to a limiting size of 0.1 mm, 1 mm, and 1 cm are shown. This spans the size regime from meteoroid dominated at 0.1 mm to man-made debris dominated at 1 cm.

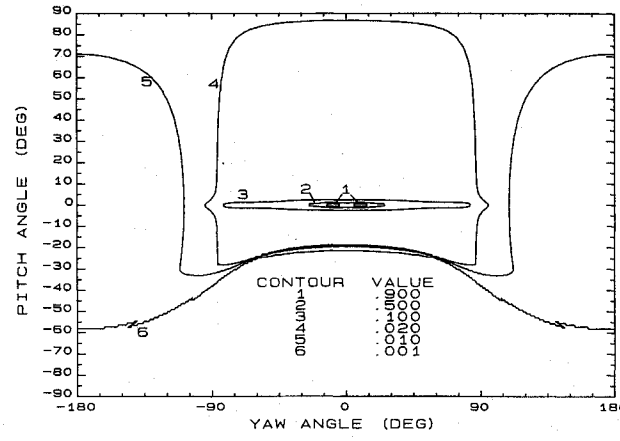

Fig. 10 Combined number flux density for 100-μ environment.

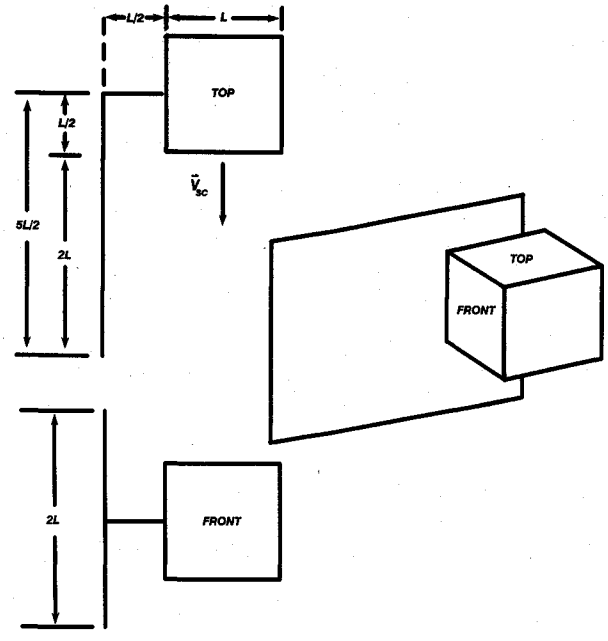

Fig. 11 Three-dimensional view of a simple spacecraft.

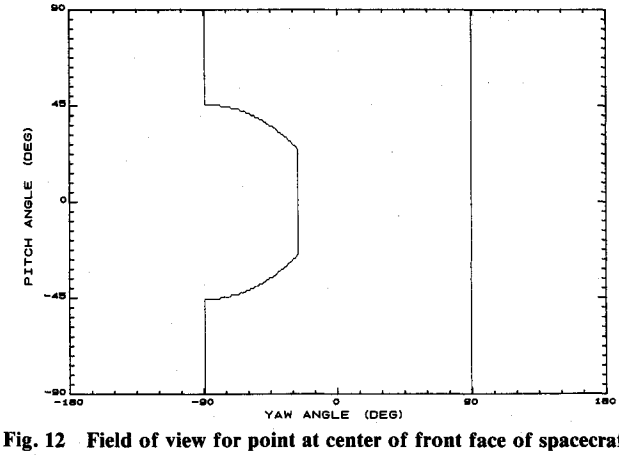

Fig. 12 Field of view for point at center of front face of spacecraft.

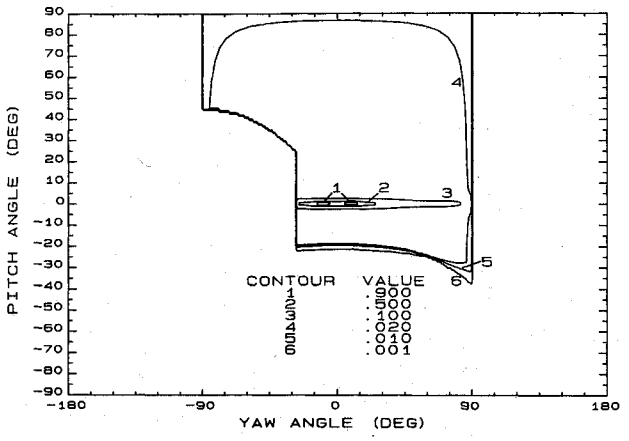

Fig. 13 Number flux density distribution for primary debris objects for point at center of front face of spacecraft.

Surface Element Shielding by Other Spacecraft Structures

A given point on the surface of a spacecraft will, in general, be shielded at least over half the sky by the structure surrounding it. If it is a simple convex structure, such as LDEF, this is the only shielding it will experience, and this case was considered in Ref. 1. Most spacecraft are more complex structures with solar panels, antennas, multiple modules, and the like that provide additional shielding from the environment at certain points on the spacecraft looking in certain directions.

When this is the case there will be no primary flux from the shielded directions and the curves shown in Figs. 1–8 will be interrupted at the outline of these structures. However, if these structures have surfaces in the line of sight to the point under consideration that are exposed to the primary debris environment, these same directions will appear as a source of secondary fragments. In fact, if the geometry is right, the secondary flux can exceed the primary flux.

A preliminary model to address these affects is presented for a generic spacecraft design shown in Fig. 11. In evaluating the masking, a point at the center of the front face was used. The mask of the structure for this point is presented in Fig. 12, where the cutout coming toward the center from a yaw of -90 deg is the projecting structure attached to the main structure. The mass flux density that this point sees is shown in Fig. 13. When this function is integrated over solid angle, a 11.6% reduction in the mass flux is found.

To calculate secondary flux levels, the mask for the extended surface would be combined with the ejecta mass flux density for the combined environments for a side looking surface to get the total amount of material coming off that surface. The flux of secondaries at another point on the spacecraft from this surface erosion will be related to the quantity of material ejected, a directional distribution relative to the surface, and the distance from the surface point.

Conclusions

A model has been presented to allow both the meteoroid and man-made debris environments to be evaluated for their effects on spacecraft surfaces. This model provides the complete size, directional, and impact velocity distributions for both populations from the phase space density distribution for the meteoroid environment and from numerical modeling for the man-made environment. In both cases, the velocity and directional distribution have been integrated over velocity and solid angle to yield fluxes onto oriented surfaces.

Since most spacecraft will be geometrically complex structures, there is a need to be able to account for shielding of a spacecraft surface by other structural elements. A approach to account for this effect within the flux density concept has been presented along with the directional distribution of primary flux for this case.

References

[1]Reynolds, R., "Man-Made Debris Environment Characterization for Spacecraft Vulnerability Assessment," *Proceedings of Space 90, Conference on Engineering, Construction, and Operations in Space,* April 1990.

[2]Southworth, R., and Sekanina, Z., "Physical and Dynamical Studies of Meteors," NASA CR-2316, 1973.

[3]Gault, D., "Displaced Mass, Depth, Diameter, and Effects of Oblique Trajectories for Impact Craters Formed in Dense Crystalline Rock," *The Moon,* Vol. 6, D. Reidel Publishing, 1973, pp. 32–44.

[4]Sawle, D., "Hypervelocity Impact in Thin Sheets and Semi-Infinite Targets at 15 km/sec," *AIAA Journal,* Vol. 8, No. 7, 1970, pp. 1240–1244.

[5]Bruce, E., "Review and Analysis of High Velocity Impact Data," *Proceedings of the Fifth Hypervelocity Impact Symposium,* Colorado School of Mines, Golden, CO, 1962, pp. 439–474.

[6]Schneider, E., "Velocity Dependence of Some Impact Phenomena," *Proceedings of the Comet Halley Micrometeoroid Hazard Workshop,* European Space Agency Scientific and Technical Publications Branch, ESA SP-153, The Netherlands, 1979, pp. 101–107.

[7]Goodman, E., and Liles, C., "Particle-Solid Impact Phenomena," *Proceedings of the Sixth Hypervelocity Impact Symposium,* Firestone Tire and Rubber Co., Akron, OH, 1963, pp. 543–577.

[8]Dunn, W., "On Material Strengths of the Hypervelocity Impact Problem," *AIAA Journal,* Vol. 4, No. 3, 1966, pp. 535–536.

[9]Christman, D., "Target Strength and Hypervelocity Impact," *AIAA Journal,* Vol. 4, No. 10, 1966, pp. 1872–1874.

[10]Herrmann, W., and Jones, A., "Correlation of Hypervelocity Impact Data," *Proceedings of the Fifth Hypervelocity Impact Symposium,* Colorado School of Mines, Golden, CO, 1962, pp. 389–438.

[11]Schonberg, W., and Taylor, R., "Exterior Spacecraft Subsystem Protective Shielding Analysis and Design," *Journal of Spacecraft and Rockets,* Vol. 27, No. 3, 1990, pp. 267–274.

[12]Zook, H., "The State of Meteoric Material on the Moon," *Proceedings of Lunar Science Conference VI,* NASA Johnson Space Center, Houston, TX, 1970, pp. 1653–1672.

[13]Zook, H., Flaherty, R., and Kessler, D., "Meteoroid Impacts on the Gemini Windows," *Planetary Space Science,* Vol. 18, 1970, pp. 953–964.

[14]Kessler, D., Reynolds, R., and Anz-Meador, P., *Orbital Debris Environment for Spacecraft Designed to Operate in Low Earth Orbit,* NASA TM 100 471, April 1989.

Antoni K. Jakubowski
Associate Editor